British Journal of Pharmacology (2009), 156, 1296–1304

0007-1188/09
www.brjpharmacol.org

RESEARCH PAPER

Amiloride derivatives induce apoptosis by depleting ER Ca^{2+} stores in vascular endothelial cells

KS Park[1,2]*, D Poburko[1]*, CB Wollheim[1] and N Demaurex[1]

[1]*Department of Cell Physiology and Metabolism, University of Geneva, Geneva, Switzerland,* [2]*Department of Physiology, Yonsei University Wonju College of Medicine, Wonju, Korea*

Background and purpose: Amiloride derivatives are blockers of the Na^+/H^+ exchanger (NHE) and at micromolar concentrations have protective effects on cardiac and brain ischaemia/reperfusion injury but at higher concentrations also induce apoptosis. Here, we aimed to elucidate the mechanism related to this cytotoxic action.
Experimental approach: We quantified the expression of genes associated with endoplasmic reticulum (ER) stress and measured changes in luminal ER Ca^{2+} concentration ($[Ca^{2+}]_{ER}$) with a 'cameleon' indicator, D1ER.
Key results: Amiloride derivatives induced apoptosis in vascular endothelial cells, an effect that increased at alkaline extracellular pH. The potency order for cytotoxicity was 5-(N,N-hexamethylene)-amiloride (HMA) > 5-(N-methyl-N-isobutyl) amiloride > 5-(N-ethyl-N-isopropyl) amiloride (EIPA) >> amiloride. HMA dose-dependently increased the transcription of the ER stress genes GADD153 and GADD34 and rapidly depleted $[Ca^{2+}]_{ER}$, mimicking the effects of the sarco/endoplasmic reticulum ATPase (SERCA) inhibitor thapsigargin. The NHE1-specific inhibitor HOE 694 inhibited NHE activity by 87% but did not alter $[Ca^{2+}]_{ER}$. The decrease in $[Ca^{2+}]_{ER}$ evoked by amiloride derivatives was also observed in HeLa cells and was mirrored by an increase in cytosolic Ca^{2+} concentration.
Conclusions and implications: Amiloride derivatives disrupt ER and cytosolic Ca^{2+} homeostasis by a mechanism unrelated to NHE inhibition, most likely by interfering with the activity of SERCA. We propose that ER Ca^{2+} depletion and subsequent ER stress provide a rationale framework for the apoptotic effects of amiloride derivatives.
British Journal of Pharmacology (2009) **156**, 1296–1304; doi:10.1111/j.1476-5381.2009.00133.x; published online 19 March 2009

Keywords: amiloride derivatives; ER stress; ER calcium depletion; D1ER; Na^+/H^+ exchanger

Abbreviations: $[Ca^{2+}]_{ER}$, ER Ca^{2+} concentration; $[Ca^{2+}]_i$, cytosolic calcium concentration; EIPA, 5-(N-ethyl-N-isopropyl) amiloride; HMA, 5-(N,N-hexamethylene)-amiloride; NHE, Na^+/H^+ exchanger; SERCA, sarco/endoplasmic reticulum ATPase

Introduction

Amiloride and a number of its derivatives are widely used as blockers of the Na^+/H^+ exchangers. Nine isotypes of the mammalian Na^+/H^+ exchanger (NHE 1-9) have been identified (Orlowski and Grinstein, 2004; Nakamura *et al.*, 2005), with NHE 1-5 located in the plasma membrane and NHE 6-9 in intracellular organelles, such as endosomes or the Golgi complex (Slepkov *et al.*, 2007). NHE inhibitors protect against ischaemia/reperfusion injury in the heart and brain (Kitayama *et al.*, 2001; Slepkov *et al.*, 2007; Javadov *et al.*, 2008), and have been tested for their potential to reduce damage during recovery from coronary artery occlusion (du Toit and Opie, 1993; Bugge *et al.*, 1996). NHE inhibitors are thought to protect brain cells from Ca^{2+} overload during reperfusion, because NHE-mediated clearance of the ischaemic acid load increases intracellular Na^+ concentration, driving the Na^+-Ca^{2+} exchanger (NCX) in the 'reverse' Ca^{2+} entry mode (Tani and Neely, 1989). However, the role of NCX in ischaemic brain injury is controversial, because the use of different ischaemia models and the lack of truly specific NCX inhibitors and activators has led to conflicting results, with some studies showing that NCX activity is neuroprotective and others neurodamaging (Jeffs *et al.*, 2007). Similarly, although animal studies clearly showed that NHE inhibition protects against cardiac ischaemic injury, clinical trials with the NHE1-specific inhibitors cariporide, eniporide and zoniporide have provided rather disappointing data and even revealed adverse effects of NHE inhibition (Avkiran *et al.*, 2008).

In contrast to their protective effects, amiloride derivatives also elicit growth inhibition and apoptotic cell death in hepatocytes (Suzuki and Tsukamoto, 2004), leukaemic cells (Rich

Correspondence: Nicolas Demaurex, 1 rue Michel-Servet, 1211-CH, Geneva, Switzerland. E-mail: Nicolas-Demaurex@medecine.unige.ch
*These authors contributed equally to this work.
Received 6 November 2008; accepted 28 November 2008

et al., 2000), smooth muscle (Chen and O'Brien, 2003) and neurons (Schneider *et al*., 2004). Based on these apoptotic effects, amiloride analogues were proposed as potential therapeutic agents against metastasis and multi-drug resistant cancers (Harguindey and Cragoe, 1992). Inhibition of Na^+-coupled H^+ efflux decreases intracellular pH (Counillon and Pouyssegur, 2000), and the subsequent cytosolic acidification can trigger apoptosis by promoting mitochondrial cytochrome c release and caspase activation (Furlong *et al*., 1997; Park *et al*., 1999; Matsuyama *et al*., 2000; Kristian *et al*., 2001). Thus, acidification induced by NHE inhibition was suggested to be the apoptogenic mechanism of amiloride derivatives (Rich *et al*., 2000; Schneider *et al*., 2004). Conversely, the characteristic cytosolic alkalinization of malignant tumour cells is in part due to growth factors and oncogenes up-regulating NHE expression (Reshkin *et al*., 2000; Cardone *et al*., 2005). In addition, the cytotoxic effects of amiloride have also been attributed to non-specific effects on the Na^+/K^+ ATPase (Renner *et al*., 1988), protein kinase C (Besterman *et al*., 1985) and protein synthesis (L'Allemain *et al*., 1984).

The vascular endothelium forms a barrier between blood and tissues, and endothelial cells are involved in many physiological processes such as controlling vascular tone, tissue growth and wound healing. However, as these cells are situated at the blood-tissue interface they are exposed to high concentrations of circulating drugs, making them a vulnerable target for the toxic side effects of therapeutic agents. In this study, we demonstrate the pro-apoptotic effects of amiloride derivatives such as 5-(N,N-hexamethylene)-amiloride (HMA) in endothelial cells, at micromolar concentrations that are close to the concentrations required to provide protection against ischaemia/reperfusion injury (Meng *et al*., 1993). Amiloride derivatives depleted endoplasmic reticulum (ER) calcium stores and increased the transcription of ER stress genes during apoptosis. We propose that ER Ca^{2+} depletion and subsequent stress is an early and important mechanism for the induction of apoptotic cell death by amiloride derivatives.

Methods

Cell culture and transfection

Human umbilical endothelial cells (HUVECs) were cultured in endothelial growth medium (EGM-2) and used between passages three to seven. Endothelial hybridoma EA.hy926 cells were cultured in Dulbecco's modified eagle medium (DMEM) (Ref no. 41965-039). HeLa cells were cultured in DMEM (Ref no. 41090-028) as described previously (Jousset *et al*., 2007). All cells were cultured at 37°C in a humidified incubator (95% air-5% CO_2).

MTT analysis

Cell survival of HUVECs was determined using a 3-(4, 5-dimethylthiazolyl-2)-2, 5-diphenyl tetrazolium bromide (MTT) colorimetric assay. HUVECs seeded on a 96-well plate (10^4 cells per well) were treated with amiloride derivatives and incubated for 24 h, followed by the addition of MTT (50 μg per well). After further incubation for 2 h, culture medium was discarded and 100 μL of dimethylsulphoxide (DMSO) was subsequently added to each well. After the plate had been shaken, absorbance of each well at 570 nm and 650 nm was measured and subtracted (A_{570}-A_{650}) by an enzyme–linked immuno sorbent assay (ELISA) reader.

Flow cytometry

Human umbilical endothelial cells were harvested, washed twice with phosphate–buffered saline (PBS) and suspended in 70% ethanol at 4°C for 2 h. Cells were then washed and resuspended in 1 mL PBS, and treated with 5 μg propidium iodide, 50 μg ribonuclease A and 0.1% triton X-100 under low light and analysed for DNA content by flow cytometry. To distinguish further apoptotic versus necrotic cell death, we treated cells with FITC-labelled annexin-V and propidium iodide (FITC apoptosis detection) as per the manufacturer's instruction, and cell labelling intensity was measured by flow cytometry.

Quantitative reverse transcription-polymerase chain reaction (RT-PCR) analysis

Total cellular RNA was isolated and purified from HUVECs using the RNeasy mini kit. RT was performed with random hexamers using reverse transcriptase. Oligonucleotide primers specific for the genes of interest were designed by Bioneer (Daejeon, Korea) based on human sequences from GenBank (Table 1). Quantitative real-time PCR using SYBR Green PCR Master mix was performed with an ABI PRISM 7900HT sequence detection system according to the manufacturer's protocol. The amplification program was: activation of

Table 1 Primers for quantitative reverse transcription-polymerase chain reaction

Genes		*Sequence (5′ to 3′)*	*Position*	*Product size (bp)*	*Gene bank accession no.*
GADD153	Sense	aat cag agc tgg aac ctg ag	74-93	108	NM_004083
	Antisense	tct ctg cag ttg gat cag tc	181-162		
GADD34	Sense	tga gac ttc tgc ttc cac ac	1488-1507	107	NM_014330
	Antisense	cct cac tat cca cat cct ca	1594-1575		
GRP78 (HSP70)	Sense	ctt atg gcc tgg ata aga gg	827-846	141	NM_005347
	Antisense	cac cca gat gag tat ctc ca	967-948		
GP96 (GRP94)	Sense	gcc tag acc agt atg tgg aa	1673-1692	150	NM_003299
	Antisense	cca cag gtt ctg tga ggt aa	1822-1803		
Cyclooxygenase-2	Sense	gag cat cta cgg ttt gct gt	933-952	106	NM_000963
	Antisense	gca cat cgc ata ctc tgt tg	1038-1019		

AmpliTaq Gold at 95°C for 10 min, followed by 45 cycles of three-step PCR with denaturation at 95°C for 30 s, annealing at 60°C for 30 s and extension at 72°C for 1 min. All amplifications were followed by melting curve analysis. As an endogenous control, β-actin was used to correct for potential variation in RNA loading or efficiency of the amplification reaction. The transcriptional levels were estimated and compared using the equation of '$2^{-\triangle\triangle Ct}$' (Livak and Schmittgen, 2001).

Calcium measurements

Ea.hy926 cells (1.5~2.0 × 10^5 cells) were plated on 25 mm glass coverslips in 35 mm cultured dishes. One day post-plating, Ea.hy926 cells were transfected with 2 μg of D1ER plasmid (Palmer *et al.*, 2004) and 3.5 μL Transfast 48 h before ER Ca^{2+} concentration ($[Ca^{2+}]_{ER}$) measurements. Cytosolic calcium concentration ($[Ca^{2+}]_i$) was measured with the YC3.6 cameleon construct (Nagai *et al.*, 2004). Experiments were performed with HEPES-buffered solution (HBSS) containing 135 mmol·L^{-1} NaCl, 3.6 mmol·L^{-1} KCl, 2 mmol·L^{-1} $NaHCO_3$, 0.5 mmol·L^{-1} NaH_2PO_4, 0.5 mmol·L^{-1} $MgSO_4$, 2 mmol·L^{-1} $CaCl_2$, 10 mmol·L^{-1} HEPES, pH 7.4. Changes in $[Ca^{2+}]_{ER}$ and $[Ca^{2+}]_i$ were monitored at 37°C as previously described (Jousset *et al.*, 2007). Ratio image pairs (excited with 430 nm) were acquired at 0.1~0.2 Hz to minimize phototoxicity.

HeLa cells were plated at 5–8 × 10^4 cells per well on 96-well plates (Ref. no. 655090), and were transfected 24–48 h later with Ca^{2+} probe (0.4 μg per well D1ER or YC3.6 plasmids) and Lipofectamine 2000 (1.28 μg per well). Cells were washed after 8~10 h transfection, and $[Ca^{2+}]_i$ and $[Ca^{2+}]_{ER}$ were measured ~48 h later. Prior to experiments, culture medium was replaced with 100 μL HBSS, and the plate was placed in a plate-reading microscope. Ratiometric image pairs were acquired for the same 3~6 locations per well with a 20× objective using CFP (λ_{ex} 435/25 nm, 465 nm dichroic, λ_{em} 480/35 nm) and FRET (λ_{ex} 435/25 nm, 465 nm dichroic, λ_{em} 535/40 nm) filter sets. After basal image pairs had been acquired, 100 μL of inhibitor or thapsigargin (2× final concentration) was added to each well, and images were collected at ~10 min intervals for ≤40 min. Custom algorithms were created in MetaXpress software to define automatically cell regions and remove background fluorescence. Using macros in Excel, single-cell mean intensity fluorescence per image (50~400 cells per well) was sorted and converted to ratio values, excluding ratios more than mean ± 2 × s.d.

Materials

Human umbilical endothelial cells were purchased from Clonetics (Ref. no. CC-2617, Cambrex BioScience, Walkersville, MD, USA); EGM-2, Bulletkit (Cambrex BioScience). Endothelial hybridoma EA.hy926 cells were a kind gift from Dr M. Frieden (University of Geneva, Switzerland). DMEM (Ref. no. 41965-039 and no. 41090-028) and Lipofectamine 2000 were purchased from Invitrogen (Basel, Switzerland); MTT and DMSO, Sigma (St. Louis, MO, USA); the ELISA reader, Molecular Devices (Sunnyvale, CA, USA). The flow cytometry used to analyse DNA content and FITC apoptosis detection kit were obtained from BD bioscience (San Jose, CA, USA); the RNeasy mini kit, Qiagen (Valencia, CA, USA); the random hexamers, Takara (Kyoto, Japan); reverse transcriptase, Promega (Madison, WI, USA); SYBR Green PCR Master mix and ABI PRISM 7900HT Sequence Detection System, Applied Biosystems (Foster, CA, USA); Transfast, Promega (Dubendorf, Switzerland). The 96-well plates (Ref. no. 655090) were from Greiner Bio-one Vacuette (Schweiz GmbH, St. Gallen, Switzerland); the plate-reading microscope (Image Xpress micro) and the MetaXpress software, Molecular Devices (Sunny Vale, CA, USA); macros in Excel, Microsoft Corporation (Redmond, WA, USA).

Data analysis

The concentration-response curves and EC_{50} values were obtained by using GraphPad Prism version 4.0 (GraphPad Software, San Diego, CA, USA). Statistical significance was determined using Student's *t*-test, and $P < 0.05$ was considered significant.

Results

Apoptotic cell death by amiloride derivatives

As shown in Figure 1A, HMA (10 μmol·L^{-1}) elicited cytosolic shrinkage and nuclear condensation of HUVECs. MTT assays revealed dose-dependent cytotoxicity after a 24 h incubation with amiloride derivatives in HUVECs (Figure 1B). The rank order of potency was HMA (IC_{50} 11.2 μmol·L^{-1}) > 5-(N-methyl-N-isobutyl) amiloride (13.6 μmol·L^{-1}) > 5-(N-ethyl-N-isopropyl) amiloride (EIPA; 30.8 μmol·L^{-1}) >> amiloride (106 μmol·L^{-1}).

Cytosolic acidification by amiloride derivatives is known to elicit cytotoxicity, which can be alleviated by maintaining cells in alkaline extracellular medium (Schneider *et al.*, 2004). To test whether the cytotoxic effects of amiloride derivatives were due to cytosolic acidification, we compared the cytotoxic effects of HMA at different extracellular pH (7.4~8.8). Intriguingly, the cell death caused by HMA increased with extracellular alkalinization, reducing cell survival by 40.2% at 7.4 but 74.6% and 91.7% at pH_o 8.1 and 8.8 (Figure 1C).

We analysed the changes in cell cycle of HMA-treated HUVECs by flow cytometry using propidium iodide to stain nuclei after fixation and permeabilization. Compared with vehicle (DMSO) application, HMA increased the proportion of cells with sub-G_0/G_1 ploidy from 4.5% of control cells to 16.3% at 10 μmol·L^{-1} and 43.2% at 30 μmol·L^{-1} HMA (Figure 2A). Consistent with these changes, the proportion of cells in mitosis (G_2/M phase) was decreased by HMA. The HMA-induced increase in sub-G_0/G_1 phase was attenuated by the non-specific caspase inhibitor, z-VAD-fmk (100 μmol·L^{-1}).

To confirm that apoptosis was the mechanism of cell death, we labelled cells with FITC apoptosis detection (Figure 2B). Untreated control cells were not stained by either agent and located in the lower left quadrant in Figure 2B. Conversely, 73.0% of cells treated with HMA for 24 h were labelled for annexin-V and not propidium iodide (apoptotic cells, lower right quadrant) with some cells also being labelled with propidium iodide indicating necrosis (upper right quadrant).

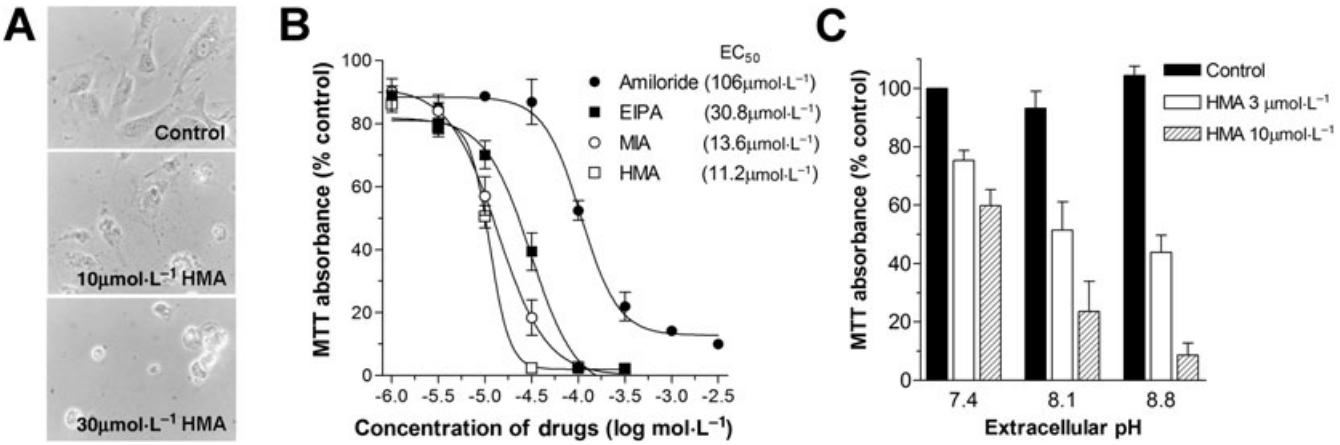

Figure 1 Cytotoxic effects of amiloride derivatives on human umbilical endothelial cells (HUVECs). (A) Micrograph (×100) of control and HMA-treated cells. HMA induced prominent cell shrinkage within 24 h. (B) Dose–response curves for cytotoxicity induced by 24 h of exposure to amiloride and its derivatives, obtained using the MTT assay. (C) Effects of alkaline extracellular pH (pH_o) on HMA-induced cytotoxicity, evaluated by the MTT assay. Data are expressed as mean ± s.e.mean (n = 6). HMA, 5-(N,N-hexamethylene)-amiloride; MTT, 3-(4, 5-dimethylthiazolyl-2)-2, 5-diphenyl tetrazolium bromide.

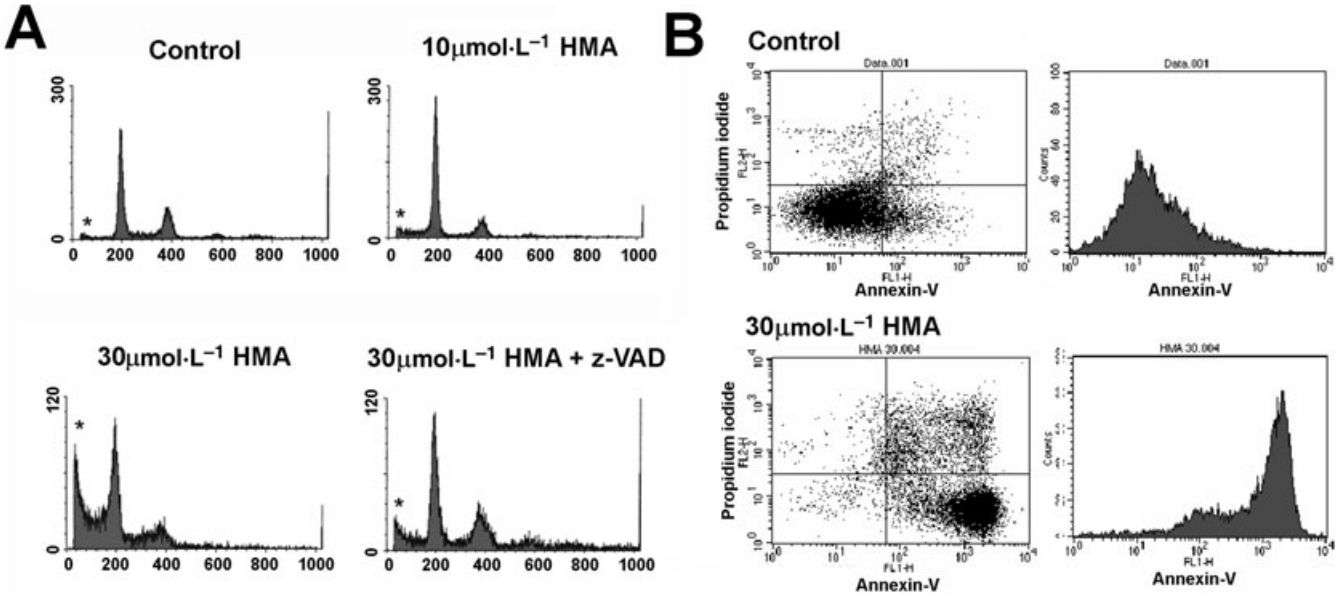

Figure 2 Changes in cell cycle and annexin-V positive cells by amiloride derivatives. (A) Cell cycle changes were measured using propidium iodide staining and flow-cytometry analysis. Asterisk (*) shows the cell number of sub-G_0/G_1 ploidy (apoptotic cells). (B) Cells were labelled with FITC-Annexin V and propidium iodide, and analysed by flow cytometry. Apoptotic cells, located at lower right quadrant, were increased by the exposure to HMA (30 μmol·L^{-1}) for 24 h (73%), compared with those of control (11.3%). HMA, 5-(N,N-hexamethylene)-amiloride.

HMA-induced ER stress

Table S1 displays the micro-array data comparing the transcriptional level of genes involved in apoptosis between control and HMA-treated (10 μmol·L^{-1} for 24 h) HUVECs. Several ER stress genes and cyclooxygenase-2 (COX-2) were significantly up-regulated in HMA-treated HUVECs. We confirmed these findings by quantitative RT-PCR for ER stress proteins and COX-2. Within 24 h, HMA greatly increased the expression of COX-2 and the ER stress proteins GADD153 and GADD34, which are known to be involved in apoptosis induced by ER stress (Figure 3). In contrast, the up-regulation of ER chaperone proteins including GRP78 and GRP94 was less prominent compared with that of pro-apoptotic growth arrest and DNA damage-inducible (GADD) proteins.

Depletion of ER Ca^{2+} stores by HMA

Endoplasmic reticulum stress is induced by Ca^{2+} depletion of the ER, a condition pharmacologically achieved with thapsigargin, an inhibitor of sarco/endoplasmic reticulum ATPase (SERCA). To test the hypothesis that amiloride derivatives caused depletion of ER Ca^{2+} stores, we directly measured $[Ca^{2+}]_{ER}$ changes in endothelial hybridoma (EA.hy926) cells

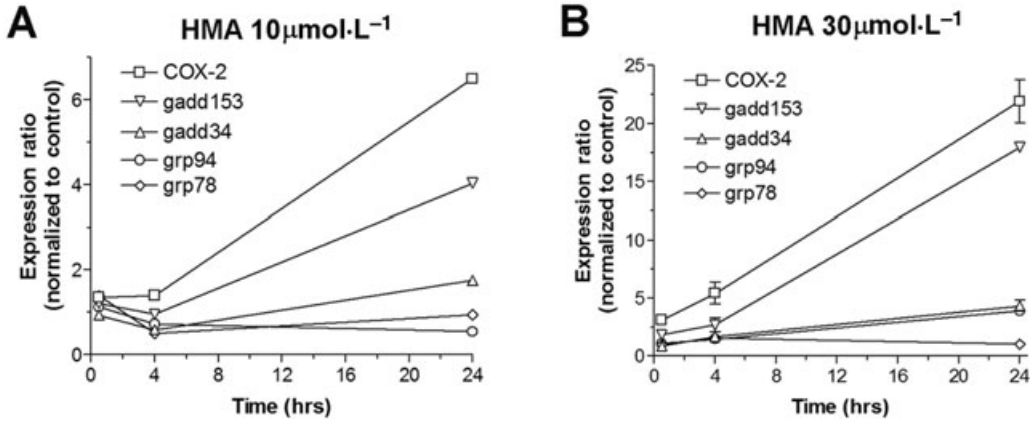

Figure 3 Expression levels of ER stress proteins following HMA treatment. Using quantitative real-time RT-PCR analysis, the transcriptional levels of cyclooxygenase-2 (COX-2) and ER stress proteins (GADD153, GADD34, GRP94 and GRP78) were measured at 30 min, 4 h and 24 h after the application of 10 μmol·L^{-1} (A) or 30 μmol·L^{-1} (B) HMA, and normalized to the expression level of the untreated group. Data are shown as mean ± s.e.mean of one to four experiments. ER, endoplasmic reticulum; HMA, 5-(N,N-hexamethylene)-amiloride; RT-PCR, reverse transcription-polymerase chain reaction.

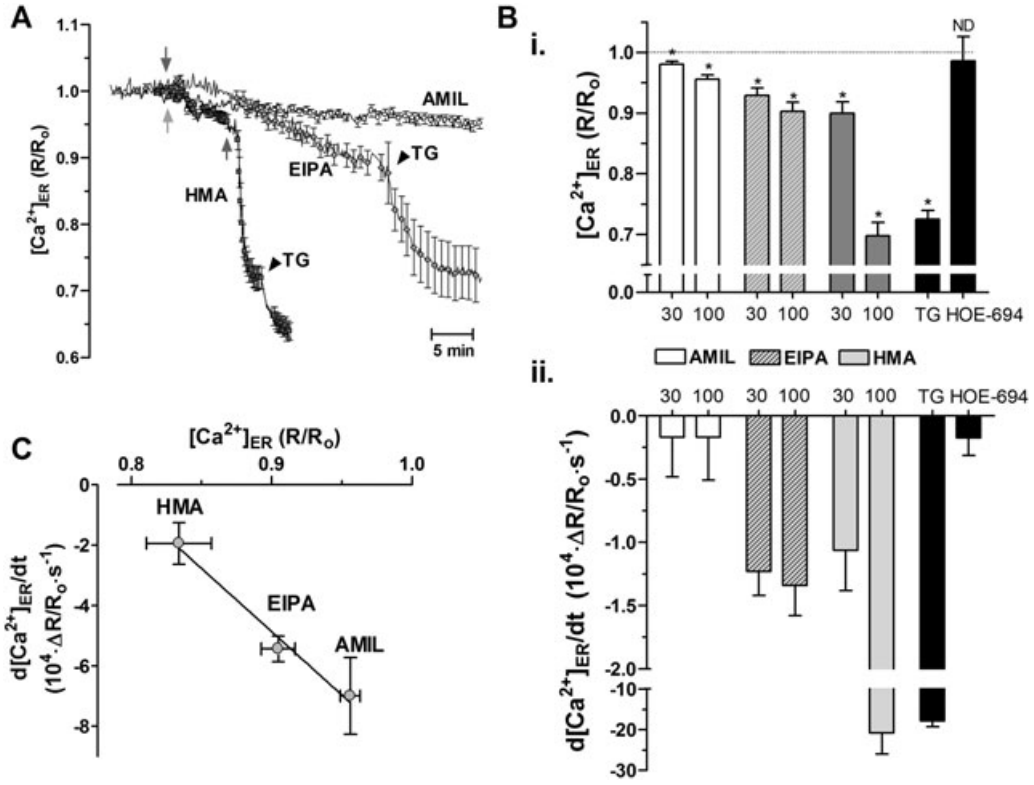

Figure 4 Kinetics and extent of ER calcium depletion by amiloride derivatives. The luminal ER calcium concentration ($[Ca^{2+}]_{ER}$) was measured in Ea.hy296 cells 48 h after transfection with the D1ER Ca^{2+} probe. Changes in $[Ca^{2+}]_{ER}$ are expressed as D1ER ratios normalized to initial values. (A) Averaged traces from individual experiments for $[Ca^{2+}]_{ER}$-depletion by HMA (average of six cells), EIPA (six cells) and amiloride (eight cells). Drug additions are: ↟ 30 μmol·L^{-1} and ↑ 100 μmol·L^{-1} HMA, ↓ 30 μmol·L^{-1} EIPA and 100 μmol·L^{-1} amiloride, ▼ 1 μmol·L^{-1} thapsigargin (TG). (B) Average degree (top; i) and rate (bottom; ii) of $[Ca^{2+}]_{ER}$ depletion from protocols in panel (A). X-axis shows consecutive addition of 30 μmol·L^{-1} and 100 μmol·L^{-1} of drug. Data are mean ± s.e.mean for 12–25 cells in three to five independent experiments. *$P < 0.05$ for 1-sample *t*-test versus (top) 1 or (bottom) 0. (C) The rate of thapsigargin-mediated ER Ca^{2+} depletion following treatment with amiloride derivatives was proportional to the extent of ER depletion at the point of thapsigargin addition. $[Ca^{2+}]_{ER}$, ER Ca^{2+} concentration; EIPA, 5-(N-ethyl-N-isopropyl) amiloride; ER, endoplasmic reticulum; HMA, 5-(N,N-hexamethylene)-amiloride.

using an ER-targeted Ca^{2+} sensor, D1ER (Palmer *et al.*, 2004). As shown in Figure 4, HMA dose-dependently decreased $[Ca^{2+}]_{ER}$, represented as the change in D1ER ratio normalized to the initial value for the ratio. Remarkably, 100 μmol·L^{-1} HMA induced a depletion of $[Ca^{2+}]_{ER}$ equivalent in amplitude and kinetics to the maximal depletion evoked by complete inhibition of SERCA with thapsigargin (Figure 4B). Thapsigargin did not further decrease $[Ca^{2+}]_{ER}$ significantly when added

after HMA (Figure S1A), demonstrating that HMA depleted the thapsigargin-sensitive ER Ca^{2+} pool. Likewise, HMA did not decrease $[Ca^{2+}]_{ER}$ when added after thapsigargin and the two compounds did not have a synergistic effect when added simultaneously (Figure S1), confirming that HMA and thapsigargin mobilize the same Ca^{2+} pool. Amiloride and EIPA also induced depletion of $[Ca^{2+}]_{ER}$, but to a lesser degree. The extents and rates of ER depletion induced by HMA > EIPA > amiloride (Figure 4B) were consistent with their rank order potency of cytotoxicity (Figure 1B). As a more selective NHE1 inhibitor, we applied a benzoylguanidine, HOE-694. By measuring the Na^+-dependent changes in intracellular pH during recovery from an acid load, we observed a marked inhibition of NHE activity with HOE-694 (87% inhibition at 1 $\mu mol \cdot L^{-1}$, Figure S2) suggesting that NHE1 is the predominant isoform in EA.hy296 cells. As shown in Figure 4B, however, a supramaximal concentration of HOE-694 (100 $\mu mol \cdot L^{-1}$) did not significantly affect $[Ca^{2+}]_{ER}$, suggesting that the changes in $[Ca^{2+}]_{ER}$ elicited by HMA in endothelial cells are not mediated by NHE1 inhibition. Addition of a lower dose of HMA (10 $\mu mol \cdot L^{-1}$) evoked significant depletion of ER Ca^{2+} (Figure S3). In this case, a subsequent addition of thapsigargin caused further depletion of $[Ca^{2+}]_{ER}$, as observed with the less potent amiloride derivatives (Figure 4A, arrowheads). This thapsigargin-induced decrease reflected the Ca^{2+} permeability of the ER, the 'Ca^{2+} leak' normally balanced by active SERCA pumping. Interestingly, the rates of thapsigargin-induced depletion of $[Ca^{2+}]_{ER}$ were directly proportional to the level of the remaining $[Ca^{2+}]_{ER}$ in cells treated with HMA, EIPA or amiloride (Figure 4C). This indicates that the Ca^{2+} leak rates were determined primarily by the Ca^{2+} gradient, regardless of the inhibitor used. HMA also increased the cytosolic Ca^{2+} concentration ($[Ca^{2+}]_i$) in EA.hy926 cells (Figure S4), consistent with Ca^{2+} release from thapsigargin-sensitive ER Ca^{2+} pool and subsequent activation of store-operated Ca^{2+} influx.

To confirm that amiloride derivatives deplete ER Ca^{2+} stores in other mammalian cell types, we measured $[Ca^{2+}]_{ER}$ and $[Ca^{2+}]_i$ in HeLa cells with the probes D1ER and $YC_{3.6}$, respectively, using a plate-reading microscope to obtain average data from transfected cell populations. The average change in $[Ca^{2+}]_i$ and $[Ca^{2+}]_{ER}$ was determined in cells exposed for 20~30 min to the inhibitors. It is noteworthy that this 'endpoint' analysis might fail to detect the transient changes in $[Ca^{2+}]_i$ evoked by amiloride derivatives (Figure S4). This high throughput image analysis revealed that, similar to endothelial cells, HMA and EIPA caused detectable elevations in $[Ca^{2+}]_i$ in HeLa cells (Figure 5A). As in Ea.hy926 cells, HMA (100 $\mu mol \cdot L^{-1}$) induced ~90% of the depletion of $[Ca^{2+}]_{ER}$ induced by thapsigargin in HeLa cells (Figure 5B). Amiloride and EIPA had a tendency to reduce D1ER ratios, but their effects were at the limit of detection in this system. These results demonstrate that disruption of ER Ca^{2+} homeostasis by amiloride derivatives is not restricted to endothelial cells.

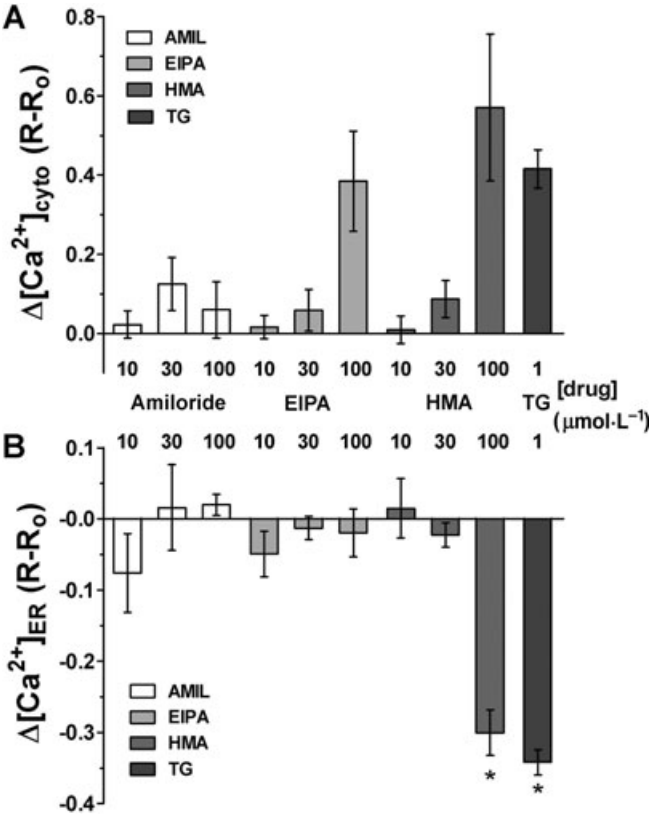

Figure 5 High throughput analysis of the ER and cytosolic Ca^{2+} changes evoked by amiloride derivatives. Relative change in $[Ca^{2+}]_i$ and $[Ca^{2+}]_{ER}$ in HeLa cells transfected with (A) YC3.6 or (B) D1ER on separate halves of 96-well plates. Each condition was repeated in duplicate and imaged in a 3~4 regions per well. Changes in ratio were calculated after 20~30 min incubation with drug or DMSO and the effect of DMSO was subtracted from the effect of each inhibitor. Columns represent mean ± s.d. from three independent experiments; each performed in duplicate, and represents the average from 60~500 cells per condition. For each replicate, the maximum (YC3.6) or minimum (D1ER) response at 20 or 30 min was taken. *$P < 0.05$ for one-sample *t*-test versus 0. $[Ca^{2+}]_{ER}$, ER Ca^{2+} concentration; $[Ca^{2+}]_i$, cytosolic calcium concentration; DMSO, dimethylsulphoxide; EIPA, 5-(N-ethyl-N-isopropyl) amiloride; HMA, 5-(N,N-hexamethylene)-amiloride; TG, thapsigargin.

Discussion

The ER is the major intracellular calcium store and the organelle responsible for the synthesis and post-translational modification of proteins. Disturbances of ER calcium homeostasis cause accumulation of unfolded or misfolded proteins in the ER lumen, leading to a variety of responses termed 'ER stress' (Ferri and Kroemer, 2001; Patil and Walter, 2001). In this study, we observed that amiloride derivatives, routinely used as NHE inhibitors, depleted ER Ca^{2+} stores and up-regulated pro-apoptotic ER stress genes in endothelial cells. We propose that ER Ca^{2+} depletion and subsequent activation of the ER stress pathway account for the apoptotic effects of amiloride derivatives.

Among amiloride derivatives, HMA was the most potent inducer of cytotoxicity in HUVECs and we thus focused on this compound. HMA induced apoptotic cell death in our hands, based on clear morphological evidence (massive cytosol shrinkage, blebbing and chromatin condensation), annexin-V labelling of phosphatidylserine and the attenuation of cell killing by a common caspase inhibitor, z-VAD-fmk. Paradoxically, we observed that HMA-induced apoptosis was enhanced at alkaline extracellular pH, a condition that

minimizes NHE activity (Slepkov *et al*., 2007). The apoptotic effects of amiloride analogues observed in this condition thus cannot be attributed to the intracellular acidification resulting from NHE inhibition, as previously suggested (Rich *et al*., 2000). In liver cells, apoptosis induced by NHE inhibitors is associated with activation of JNK kinase (Suzuki and Tsukamoto, 2004) or with the inhibition of ERK kinase (Konstantinidis *et al*., 2006). We did not detect significant changes in mitogen-activated protein (MAP) kinase activation upon exposure (1, 2 and 6 h) of HUVEC to 30 $\mu mol \cdot L^{-1}$ HMA (Figure S5), indicating that the apoptotic effects of amiloride derivatives were independent of the MAP kinase pathway.

Cyclooxygenase-2 was the gene most markedly up-regulated in our microarray screening assay of HUVECs treated with HMA. COX-2 produces prostaglandin E_2 for autocrine or paracrine signalling, but unlike COX-1 that is ubiquitous and constitutively expressed, COX-2 is absent from endothelial cells and white blood cells that have not been exposed to noxious stimuli such as inflammatory cytokines (Jones *et al*., 1993), lipopolysaccharide and phorbol myristate acetate (Hla and Neilson, 1992). This suggests that HMA treatment mimics the effects of noxious stimuli that induce COX-2 expression in endothelial cells, potentially leading to the generation of PGE_2 that might impact on the vascular permeability *in vivo*.

Our first hint that the mechanism of apoptosis induced by HMA involved the ER was the up-regulation of several ER stress-related genes. Two GADD proteins were up-regulated as well as two ER chaperones, GRP94 and GRP78/BiP. Up-regulation of GADD proteins characterizes ER stress-mediated apoptosis (Eymin *et al*., 1997; Zinszner *et al*., 1998), while the up-regulation of chaperones indicates activation of the unfolded protein response (UPR), a controlled transcriptional response induced by ER stress (Hamman *et al*., 1998). Depletion of ER Ca^{2+} stores with thapsigargin, a well-characterized method to experimentally induce ER stress-mediated apoptosis, induces a 20- to 200-fold up-regulation of GADD34 and GADD153/CHOP (Mengesdorf *et al*., 2001). The pronounced increases in the expression levels of pro-apoptotic GADD34 and GADD153 induced by HMA (30 $\mu mol \cdot L^{-1}$) were comparable to previously reported increases observed with thapsigarin and were considerably greater than the concomitant increases in expression of anti-apoptotic chaperone proteins GRP78 and GRP94. These findings strongly suggest that amiloride derivatives elicit sufficient ER stress to evoke apoptosis, mimicking the effects of thapsigargin. Direct $[Ca^{2+}]_{ER}$ measurements confirmed that amiloride and its derivatives caused ER depletion, and revealed that the extent of cell killing by each drug was closely associated with the extent of $[Ca^{2+}]_{ER}$ depletion. Two basic mechanisms can account for the decrease in $[Ca^{2+}]_{ER}$ evoked by amiloride and its derivatives: a reduced pumping activity by SERCA or an increase in the Ca^{2+} permeability of the ER, the 'Ca^{2+} leak'. To distinguish between these two possibilities, we measured the ER Ca^{2+} leak rates after adding thapsigargin to inhibit fully SERCA. Regardless of the amiloride derivative applied, the Ca^{2+} leak rates were directly proportional to $[Ca^{2+}]_{ER}$ (Figure 4A). This indicates that the Ca^{2+} leak was determined primarily by the trans-membrane ER Ca^{2+} gradient, implying that the Ca^{2+} permeability of the ER was similar in all conditions. The effects of amiloride derivatives are thus best explained by an inhibition of SERCA, rather than by alterations in the Ca^{2+} permeability of the ER. Because Ca^{2+} pumping by P-type Ca^{2+} ATPases is coupled with proton antiport (Olesen *et al*., 2004), the decrease in SERCA activity might reflect the accumulation of cytosolic H^+ due to inhibition of plasmalemmal NHEs. However, this mechanism is difficult to reconcile with (i) the rapid effects of amiloride derivatives, which decreased $[Ca^{2+}]_{ER}$ immediately upon application; (ii) the different potency of the three inhibitors, which induce a similar acidification but depleted the ER to different extents; (iii) the lack of significant $[Ca^{2+}]_{ER}$ depletion evoked by a more selective inhibitor (HOE-694) of NHE 1, a major isoform of plasmalemmal NHE in endothelial cells (Zerbini *et al*., 1995); and (iv) the increased cytotoxicity of HMA at alkaline pH, a condition that favours cytosolic alkalinization. An alternative explanation for the latter effect is that alkaline extracellular pH increases the membrane permeability of amiloride derivatives by neutralizing the positive charge (pKa of 8.7) on their pyrazine ring (Wakabayashi *et al*., 1997), enhancing the binding of NHE inhibitors to intracellular target(s). These observations suggest that the cytotoxic effects of amiloride derivatives are not due to alterations in pH homeostasis, but to the direct action of amiloride analogues on molecules critical for the activity of SERCA and thus for ER Ca^{2+} homeostasis.

In summary, we have shown that amiloride derivatives decrease $[Ca^{2+}]_{ER}$ and increase $[Ca^{2+}]_i$ in endothelial cells and in HeLa cells. This disruption of Ca^{2+} homeostasis combined with up-regulation of ER stress-related proteins provides strong evidence that amiloride and its derivatives induce apoptosis by depleting ER Ca^{2+} stores and activating the ER stress response. Our observations provide a rationale framework for the toxic effects of high concentrations of NHE inhibitors and may account for the inhibition of angiogenesis (Alliegro *et al*., 1993; Miternique-Grosse *et al*., 2006) and for the delayed neovascularization (Sood *et al*., 1999) caused by amiloride and other K^+-sparing diuretics. Future studies are required to determine the target and the precise mechanism by which these drugs deplete intracellular Ca^{2+} stores.

Acknowledgements

We are grateful to Cyril Castelbou and Dr Maud Frieden for D1ER experiments and interpretation. We thank to Drs S. A. Jo and M. J. Kim (Korean NIH) for Western blotting of MAP kinases, and to Drs A. Palmer and R. Y. Tsien for providing the D1ER construct. This work was supported by the Swiss National Science Foundation (Grant 31-068317.02), and a grant from the Korea Research Foundation (KRF-2004-002-E00015 and -2006-013-E00082). DP was partially funded by the Canadian Natural Sciences and Engineering Research Council.

Conflict of interest

The authors state no conflict of interest.

References

Alliegro MC, Alliegro MA, Cragoe EJ Jr, Glaser, BM (1993). Amiloride inhibition of angiogenesis in vitro. *J Exp Zool* **267**: 245–252.

Avkiran M, Cook AR, Cuello F (2008). Targeting Na^+/H^+ exchanger regulation for cardiac protection: a RSKy approach? *Curr Opin Pharmacol* **8**: 133–140.

Besterman JM, May WS Jr, LeVine H 3rd, Cragoe EJ Jr, Cuatrecasas, P (1985). Amiloride inhibits phorbol ester-stimulated Na^+/H^+ exchange and protein kinase C. An amiloride analog selectively inhibits Na^+/H^+ exchange. *J Biol Chem* **260**: 1155–1159.

Bugge E, Munch-Ellingsen J, Ytrehus K (1996). Reduced infarct size in the rabbit heart in vivo by ethylisopropyl-amiloride. A role for Na^+/H^+ exchange. *Basic Res Cardiol* **91**: 203–209.

Cardone RA, Casavola V, Reshkin SJ (2005). The role of disturbed pH dynamics and the Na^+/H^+ exchanger in metastasis. *Nat Rev Cancer* **5**: 786–795.

Chen YX, O'Brien ER (2003). Ethyl isopropyl amiloride inhibits smooth muscle cell proliferation and migration by inducing apoptosis and antagonizing urokinase plasminogen activator activity. *Can J Physiol Pharmacol* **81**: 730–739.

Counillon L, Pouyssegur J (2000). The expanding family of eucaryotic Na^+/H^+ exchangers. *J Biol Chem* **275**: 1–4.

Eymin B, Dubrez L, Allouche M, Solary E (1997). Increased gadd153 messenger RNA level is associated with apoptosis in human leukemic cells treated with etoposide. *Cancer Res* **57**: 686–695.

Ferri KF, Kroemer G (2001). Organelle-specific initiation of cell death pathways. *Nat Cell Biol* **3**: E255–E263

Furlong IJ, Ascaso R, Lopez Rivas A, Collins MK (1997). Intracellular acidification induces apoptosis by stimulating ICE-like protease activity. *J Cell Sci* **110** (Pt 5): 653–661.

Hamman BD, Hendershot LM, Johnson AE (1998). BiP maintains the permeability barrier of the ER membrane by sealing the lumenal end of the translocon pore before and early in translocation. *Cell* **92**: 747–758.

Harguindey S, Cragoe EJ Jr (1992). The Na^+/H^+ antiporter in oncology in the light of the spontaneous regression of cancer and cell metabolism. *Med Hypotheses* **39**: 229–237.

Hla T, Neilson K (1992). Human cyclooxygenase-2 cDNA. *Proc Natl Acad Sci USA* **89** (16): 7384–7388.

Javadov S, Choi A, Rajapurohitam V, Zeidan A, Basnakian AG, Karmazyn M (2008). NHE-1 inhibition-induced cardioprotection against ischaemia/reperfusion is associated with attenuation of the mitochondrial permeability transition. *Cardiovasc Res* **77**: 416–424.

Jeffs GJ, Meloni BP, Bakker AJ, Knuckey NW (2007). The role of Na^+/Ca^{2+} exchanger (NCX) in neurons following ischemia. *J Clin Neurosci* **14** (6): 507–514.

Jones DA, Carlton DP, McIntyre TM, Zimmerman GA, Prescott SM (1993). Molecular cloning of human prostaglandin endoperoxide synthase type II and demonstration of expression in response to cytokines. *J Biol Chem* **268** (12): 9049–9054.

Jousset H, Frieden M, Demaurex N (2007). STIM1 knockdown reveals that store-operated Ca^{2+} channels located close to sarco/endoplasmic Ca^{2+} ATPases (SERCA) pumps silently refill the endoplasmic reticulum. *J Biol Chem* **282**: 11456–11464.

Kitayama J, Kitazono T, Yao H, Ooboshi H, Takaba H, Ago T *et al*. (2001). Inhibition of Na^+/H^+ exchanger reduces infarct volume of focal cerebral ischemia in rats. *Brain Res* **922**: 223–228.

Konstantinidis D, Koliakos G, Vafia K, Liakos P, Bantekas C, Trachana V *et al*. (2006). Inhibition of the Na^+-H^+ exchanger isoform-1 and the extracellular signal-regulated kinase induces apoptosis: a time course of events. *Cell Physiol Biochem* **18**: 211–222.

Kristian T, Bernardi P, Siesjo BK (2001). Acidosis promotes the permeability transition in energized mitochondria: implications for reperfusion injury. *J Neurotrauma* **18**: 1059–1074.

L'Allemain G, Franchi A, Cragoe E Jr, Pouyssegur J (1984). Blockade of the Na^+/H^+ antiport abolishes growth factor-induced DNA synthesis in fibroblasts. Structure-activity relationships in the amiloride series. *J Biol Chem* **259**: 4313–4319.

Livak KJ, Schmittgen TD (2001). Analysis of relative gene expression data using real-time quantitative PCR and the $2^{(-\Delta\Delta C_T)}$ Method. *Methods* **25**: 402–408.

Matsuyama S, Llopis J, Deveraux QL, Tsien RY, Reed JC (2000). Changes in intramitochondrial and cytosolic pH: early events that modulate caspase activation during apoptosis. *Nat Cell Biol* **2**: 318–325.

Meng HP, Maddaford TG, Pierce GN (1993). Effect of amiloride and selected analogues on postischemic recovery of cardiac contractile function. *Am J Physiol* **264**: H1831–H1835.

Mengesdorf T, Althausen S, Oberndorfer I, Paschen W (2001). Response of neurons to an irreversible inhibition of endoplasmic reticulum Ca^{2+}-ATPase: relationship between global protein synthesis and expression and translation of individual genes. *Biochem J* **356**: 805–812.

Miternique-Grosse A, Griffon C, Siegel L, Neuville A, Weltin D, Stephan D (2006). Antiangiogenic effects of spironolactone and other potassium-sparing diuretics in human umbilical vein endothelial cells and in fibrin gel chambers implanted in rats. *J Hypertens* **24**: 2207–2213.

Nagai T, Yamada S, Tominaga T, Ichikawa M, Miyawaki A (2004). Expanded dynamic range of fluorescent indicators for Ca^{2+} by circularly permuted yellow fluorescent proteins. *Proc Natl Acad Sci USA* **101**: 10554–10559.

Nakamura N, Tanaka S, Teko Y, Mitsui K, Kanazawa H (2005). Four Na^+/H^+ exchanger isoforms are distributed to Golgi and post-Golgi compartments and are involved in organelle pH regulation. *J Biol Chem* **280**: 1561–1572.

Olesen C, Sorensen TL, Nielsen RC, Moller JV, Nissen P (2004). Dephosphorylation of the calcium pump coupled to counterion occlusion. *Science* **306**: 2251–2255.

Orlowski J, Grinstein S (2004). Diversity of the mammalian sodium/proton exchanger SLC9 gene family. *Pflugers Arch* **447**: 549–565.

Palmer AE, Jin C, Reed JC, Tsien RY (2004). Bcl-2-mediated alterations in endoplasmic reticulum Ca^{2+} analyzed with an improved genetically encoded fluorescent sensor. *Proc Natl Acad Sci USA* **101**: 17404–17409.

Park HJ, Lyons JC, Ohtsubo T, Song CW (1999). Acidic environment causes apoptosis by increasing caspase activity. *Br J Cancer* **80**: 1892–1897.

Patil C, Walter P (2001). Intracellular signaling from the endoplasmic reticulum to the nucleus: the unfolded protein response in yeast and mammals. *Curr Opin Cell Biol* **13**: 349–355.

Renner EL, Lake JR, Cragoe EJ Jr, Scharschmidt BF (1988). Amiloride and amiloride analogs inhibit Na^+/K^+-transporting ATPase and Na^+-coupled alanine transport in rat hepatocytes. *Biochim Biophys Acta* **938**: 386–394.

Reshkin SJ, Bellizzi A, Caldeira S, Albarani V, Malanchi I, Poignee M *et al*. (2000). Na^+/H^+ exchanger-dependent intracellular alkalinization is an early event in malignant transformation and plays an essential role in the development of subsequent transformation-associated phenotypes. *FASEB J* **14**: 2185–2197.

Rich IN, Worthington-White D, Garden OA, Musk P (2000). Apoptosis of leukemic cells accompanies reduction in intracellular pH after targeted inhibition of the Na^+/H^+ exchanger. *Blood* **95**: 1427–1434.

Schneider D, Gerhardt E, Bock J, Muller MM, Wolburg H, Lang F *et al*. (2004). Intracellular acidification by inhibition of the Na^+/H^+-exchanger leads to caspase-independent death of cerebellar granule neurons resembling paraptosis. *Cell Death Differ* **11**: 760–770.

Slepkov ER, Rainey JK, Sykes BD, Fliegel L (2007). Structural and functional analysis of the Na^+/H^+ exchanger. *Biochem J* **401**: 623–633.

Sood AK, Gupta B, Chugh P (1999). Topical amiloride accelerates healing and delays neovascularization in mechanically produced corneal ulcers in rabbits. *Methods Find Exp Clin Pharmacol* **21**: 491–497.

Suzuki T, Tsukamoto I (2004). Apoptosis induced by 5-(N,N-hexamethylene)-amiloride in regenerating liver after partial hepatectomy. *Eur J Pharmacol* **503**: 1–7.

Tani M, Neely JR (1989). Role of intracellular Na^+ in Ca^{2+} overload and depressed recovery of ventricular function of reperfused ischemic rat hearts. Possible involvement of H^+-Na^+ and Na^+-Ca^{2+} exchange. *Circ Res* **65**: 1045–1056.

du Toit EF, Opie LH (1993). Role for the Na^+/H^+ exchanger in reperfusion stunning in isolated perfused rat heart. *J Cardiovasc Pharmacol* **22**: 877–883.

Wakabayashi S, Shigekawa M, Pouyssegur J (1997). Molecular physiology of vertebrate Na^+/H^+ exchangers. *Physiol Rev* **77**: 51–74.

Zerbini G, Roth T, Podesta F, Cagliero E, Doria A, Canessa M *et al*. (1995). Activity and expression of the Na^+/H^+ exchanger in human endothelial cells cultured in high glucose. *Diabetologia* **38** (7): 785–791.

Zinszner H, Kuroda M, Wang X, Batchvarova N, Lightfoot RT, Remotti H *et al*. (1998). CHOP is implicated in programmed cell death in response to impaired function of the endoplasmic reticulum. *Genes Dev* **12**: 982–995.

Supporting Information

Additional Supporting Information may be found in the online version of this article:

Figure S1 HMA and thapsigargin-induced ER Ca^{2+} depletion. Changes in $[Ca^{2+}]_{ER}$ evoked by the sequential addition of 100 μmol·L^{-1} HMA and 1 μmol·L^{-1} thapsigargin (A, B), by thapsigargin alone (C), and by the combination of both agents (D) in Ea.hy296 cells. $[Ca^{2+}]_{ER}$ is expressed as D1ER ratios normalized to initial values, with mean ± s.e.mean superimposed. These data show that HMA and thapsigargin mobilize the same Ca^{2+} pool. $[Ca^{2+}]_{ER}$, ER Ca^{2+} concentration; ER, endoplasmic reticulum; HMA, 5-(N,N-hexamethylene)-amiloride.

Figure S2 Inhibition of Na^+/H^+ exchange (NHE) activity by HMA and HOE-694. The activity of NHE was measured in Ea.hy296 cells using the pH-sensitive indicator BCECF. After acid loading with ammonium chloride, Na^+-dependent pH recovery was measured before and after addition of 30 nmol·L^{-1} HMA (A) or of the NHE1-specific inhibitor HOE-694 (B). Note that, at this very low concentration, HMA also preferentially inhibits the NHE1 isoform. HMA, 5-(N,N-hexamethylene)-amiloride.

Figure S3 ER Ca^{2+} depletion during long-term exposure to 10 μmol·L^{-1} HMA. The effects of a low dose of HMA (10 μmol·L^{-1}) on $[Ca^{2+}]_{ER}$ were measured for 50 min in Ea.hy296 cells. $[Ca^{2+}]_{ER}$ is expressed as D1ER ratio normalized to initial values, with mean ± s.e.mean superimposed. $[Ca^{2+}]_{ER}$, ER Ca^{2+} concentration; ER, endoplasmic reticulum; HMA, 5-(N,N-hexamethylene)-amiloride.

Figure S4 HMA increased cytosolic Ca^{2+} ($[Ca^{2+}]_i$) concentration. $[Ca^{2+}]_i$ was measured in Ea.hy296 cells 48 h after transfection with the YC3.6 probe. The effects of increasing concentrations of HMA on $[Ca^{2+}]_i$ are shown. $[Ca^{2+}]_i$, cytosolic calcium concentration; HMA, 5-(N,N-hexamethylene)-amiloride.

Figure S5 HMA did not alter the signalling of mitogen-activated protein (MAP) kinases. HUVECs were treated with HMA 30 μmol·L^{-1} for 0.5, 1, 2 and 6 h, and Western blotting was performed using antibodies to MAP kinases (JNK, p38 kinase and ERK) and their phosphorylated form. HMA, 5-(N,N-hexamethylene)-amiloride; HUVECs, human umbilical endothelial cells.

Table S1 Microarray data in HMA-treated HUVECs

Please note: Wiley-Blackwell are not responsible for the content or functionality of any supporting materials supplied by the authors. Any queries (other than missing material) should be directed to the corresponding author for the article.